Gas-Phase Pyrolysis Mechanisms of 3-Anilino-1-Propanol: Density Functional Theory Study

ARTICLE *in* INTERNATIONAL JOURNAL OF QUANTUM CHEMISTRY · JANUARY 2009

Impact Factor: 1.43 · DOI: 10.1002/qua.21924

6 AUTHORS, INCLUDING:

Donghui Wei
Zhengzhou University
65 PUBLICATIONS **512** CITATIONS
SEE PROFILE

HongMing Wang
Nanchang University
63 PUBLICATIONS **420** CITATIONS
SEE PROFILE

Gas-Phase Pyrolysis Mechanisms of 3-Anilino-1-Propanol: Density Functional Theory Study

JING ZHAO, MING-SHENG TANG, DONG-HUI WEI, CHU-FENG ZHAO, WEN-JING ZHANG, HONG-MING WANG

Department of Chemistry, Center of Computational Chemistry, Zhengzhou University, Zhengzhou 450052, China

Received 28 May 2008; accepted 27 August 2008
Published online 14 November 2008 in Wiley InterScience (www.interscience.wiley.com).
DOI 10.1002/qua.21924

ABSTRACT: The gas-phase pyrolytic decomposition mechanisms of 3-anilino-1-propanol with the products of aniline, ethylene, and formaldehyde or *N*-methyl aniline and aldehyde were studied by density functional theory. The geometries of the reactant, transition states, and intermediates were optimized at the B3LYP/6-31G (d, p) level. Vibration analysis was carried out to confirm the transition state structures, and the intrinsic reaction coordinate method was performed to search the minimum energy path. Four possible reaction channels are shown, including two concerted reactions of direct pyrolytic decomposition and two indirect channels in which the reactant first becomes a ring-like intermediate, followed by concerted pyrogenation. One of the concerted reactions in the direct pyrolytic decomposition has the lowest activation barrier among all the four channels, and so, it occurs more often than others. The results appear to be consistent with the experimental outcomes. Int J Quantum Chem 109: 1036–1044, 2009

Key words: density functional theory; 3-anilino-1-propanol; reaction mechanism

Introduction

The α- and β-(*N*-arylamino) propanoic acids, carboxylic acids, and 3-amino propyl alcohols are all important *materia medicas* in medicine, and they also have very broad applications in many other fields [1–4]. Al-Awadi and coworkers have reported that the gas-phase pyrolysis mechanisms of these compounds are similar [5–8]. For example, the pyrolysate of 2-*N*-arylaminopropanoic acid showed the elimination products to be CO, CH_3CHO, and aniline, while the pyrolysate of 3-*N*-arylaminopropanoic acid revealed the formation of acylic acid on aniline [6]. Since the 1990s, there has been increscent interest in the study of their synthesis, and remarkable achievements have been

Correspondence to: M.-S. Tang; e-mail: mstang@zzu.edu.cn or H.-M. Wang; e-mail: hmwang06@163.com

made. However, the pyrolytic decomposition mechanisms of these compounds have not been studied. We think it is well worthy of using the calculation method to investigate their gas-phase pyrolytic decomposition mechanisms.

3-Anilino-1-propanol is one kind of the 3-amino propyl alcohols. Al-Awadi and coworkers have confirmed that the gas-phase pyrolysis of 3-amino propyl alcohols is a concerted reaction [5], but Chen et al. have reported that the activation energy barrier of the direct concerted reaction is higher than that of nonconcerted reaction pathway [9–11]. Therefore, the other step-by-step nonconcerted reaction channel may exist and be possible to make activation energy barrier of the rate-determining step lower on the potential energy profile. We think it is an issue worth well to be explored whether there is truly a step-by-step nonconcerted reaction channel and whether this nonconcerted channel is a more energy favorable reaction pathway. This article speculates and confirms the reaction mechanisms of the 3-anilino-1-propanol's gas-phase pyrolysis by theoretical quantum chemical calculation method.

In this project, the title compound R (3-anilino-1-propanol, structure shown in Scheme 1) has been chosen as the object of investigation, and the pyrolysis mechanisms in the different reaction channels were studied using density functional theory.

Computational Details

Using density functional theory, the geometries of the reactant, transition states, intermediates, and products in all reaction channels were optimized at the B3LYP/6-31G (d, p) [12–14] level. The corresponding vibrational frequencies were calculated at the same level to take account of the zero-point vibrational energy (ZPE) and to identify the transition structures, and at the same time, the structures of intermediates and the transition states were confirmed by using the intrinsic reaction coordinate. All the theoretical calculations were performed using the Gaussian 03 [15] suits of programs.

Results and Discussion

The pyrolysates of reactant R are shown to be aniline, ethylene, and formaldehyde or *N*-methyl aniline and aldehyde, and this process could be illustrated as follows:

According to the structure of R (see Fig. 1), we undertook calculations using the Gaussian program to investigate the mechanism for this reaction and designed four possible reaction channels by two kinds of products. In the four channels, the products of channels 1 and 2 are same, while the products of channels 3 and 4 are same (shown in Scheme 1).

REACTION CHANNEL 1

As it is shown in Figure 1, reactant R pyrolytically decomposes into P1, P2, and P3 by traversing TS1 in channel 1. During this thermolytic process, three single-bonds O(5)—H(6), N(1)—C(2), C(3)—C(4) break, one single-bond N(1)—H(6), and two double-bonds C(2)—C(3), C(4)—O(5) formed

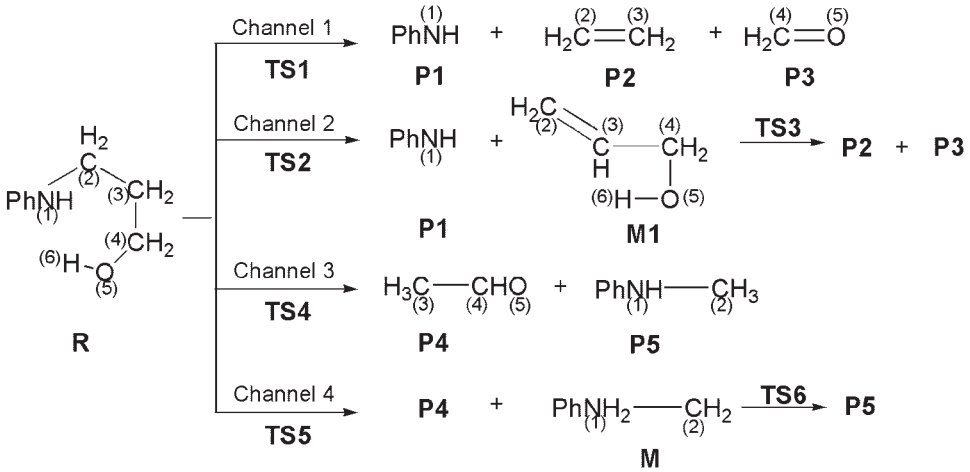

SCHEME 1. Mechanism for the pyrolytic reaction.

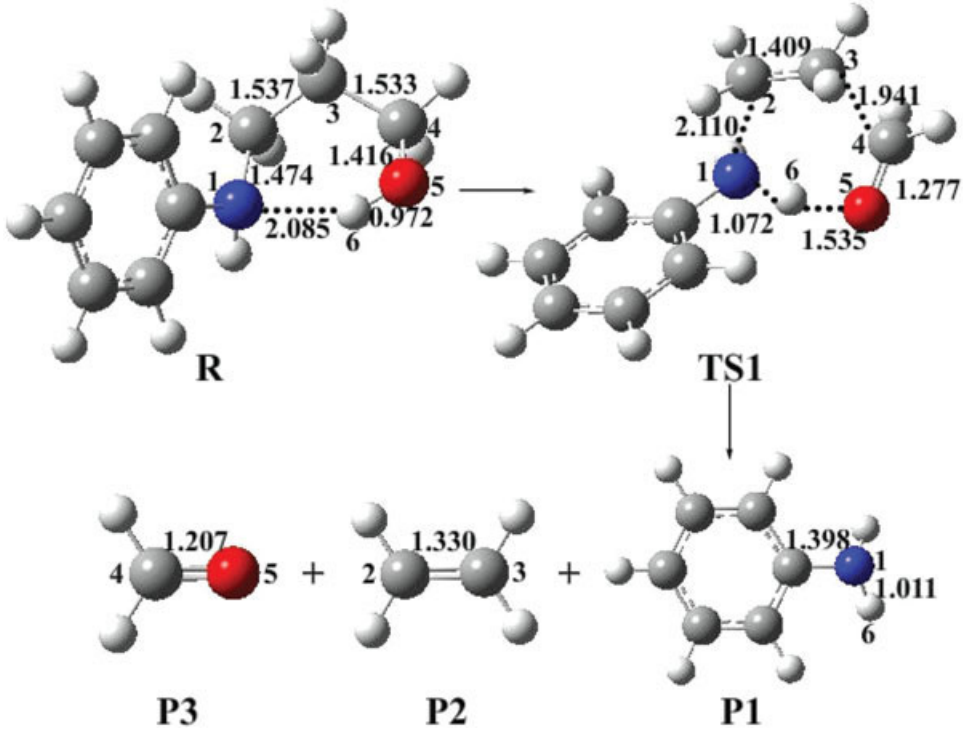

FIGURE 1. The structures and the geometrical parameters of the reactant, transition state, and products optimized at the B3LYP/6-31G (d, p) level in channel 1 (bond length in Å).

simultaneously. In other words, there are three ó bonds break so as to generate one new ó bond and two Ï bonds. With our calculated results, this process is a one-step concerted reaction. The bond lengths of the N(1)—C(2), C(3)—C(4), O(5)—H(6), N(1)—H(6),C(2)—C(3), and C(4)—O(5) change from 1.474, 1.533, 0.972, 2.085, 1.537, and 1.416 Å in R to 2.110, 1.941, 1.535, 1.072, 1.409, and 1.277 Å in TS1, respectively (shown in Fig. 1). The activation energy barrier of channel 1 is 54.48 kcal/mol at B3LYP/6-31G (d, p) level (shown in Fig. 2), and this explains why the reaction could occur at high temperature only, which is consistent with the literature reports [5–8].

REACTION CHANNEL 2

The potential energy profile of reaction channel 2 is shown in Figure 4. First, reactant R pyrolytically decomposes into P1 and intermediate M1 by traversing TS2, and then M1 converts into P2 and P3 by traversing TS3. In channel 2, first, the N(1)—C(2) and C(3)—H(9) bond lengths increase, whereas N(1) and H(9) atoms combine together to produce P1, and the C(2)═C(3) bond forms to produce M1. The bond lengths of the N(1)—C(2), C(3)—H(9), N(1)—H(9), and C(2)—C(3) change from 1.474, 1.096, 2.835, and 1.537 Å in R to 1.678, 1.691, 1.175, and 1.473 Å in TS2, respectively (shown in Fig. 3), and the activation energy barrier of this step is 70.70 kcal/mol at B3LYP/6-31G (d, p) level (shown in Fig. 4). Second, the O(5)—H(6) and C(3)—C(4) of intermediate M1 break, while with the C(3)—H(6) and C(4)═O(5) bonds combining concurrently. The bond lengths of the O(5)—H(6), C(3)—C(4), C(3)—H(6), and C(4)—O(5) change from 0.966, 1.505, 2.642, and 1.427 Å in M1 to 1.716, 1.588, 1.173, and 1.352 Å in TS3, respectively (shown in Fig. 3). The activation energy barrier of H(6) transferring from O(5) to C(3) and C(3)—C(4) bond synergize being broken to P2 and P3 by M1 traversing TS3 is 77.03 kcal/mol (see Fig. 4). Obviously, the energy barrier though this reaction channel is higher than channel 1 in which the step of H(6) transferring and N(1)—C(2), C(3)—C(4) bonds being broken happen synchronously, which shows that the activation energy barrier of the step-by-step nonconcerted reaction should not be lower than the one-step concerted reaction what we conferred [12–14]. Compared with reaction channel 2, the reaction channel 1 has more advantages.

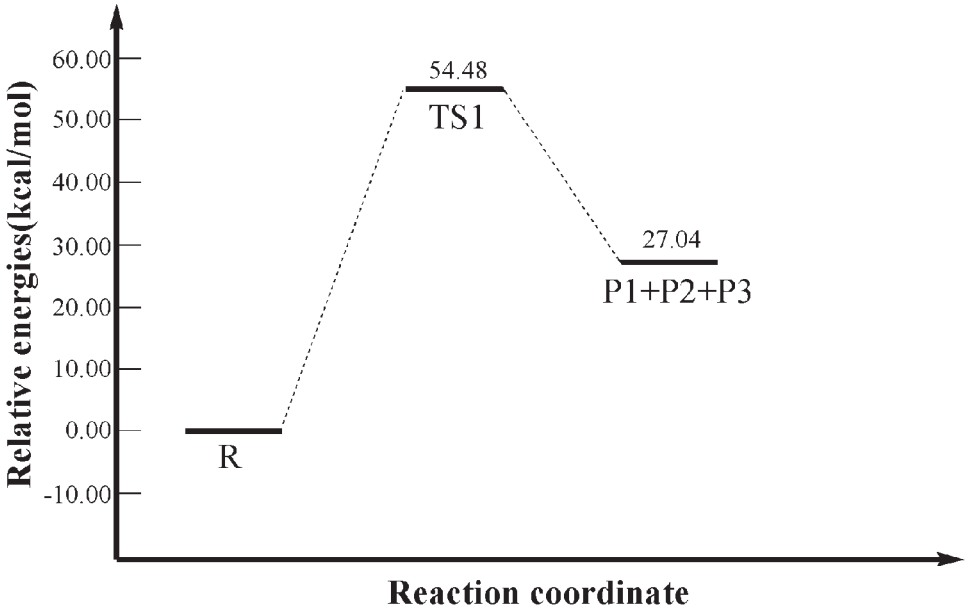

FIGURE 2. The potential energy profile of channel 1.

REACTION CHANNEL 3

As it can be seen from Figure 5, reactant R pyrolytically decomposes into P4 and P5 by traversing TS4 in channel 3. Three single-bonds C(2)—C(3), C(4)—H(11) and O(5)—H(6) break, and two single-bonds C(2)—H(6) and C(3)—H(11) form in this process. The bond lengths of the C(2)—C(3), C(4)—H(11), O(5)—H(6), C(2)—H(6), and C(3)—H(11) change from 1.537, 1.096, 0.972, 2.666, and 2.164 Å in R to 2.540, 1.138, 1.416, 1.235, and 1.917

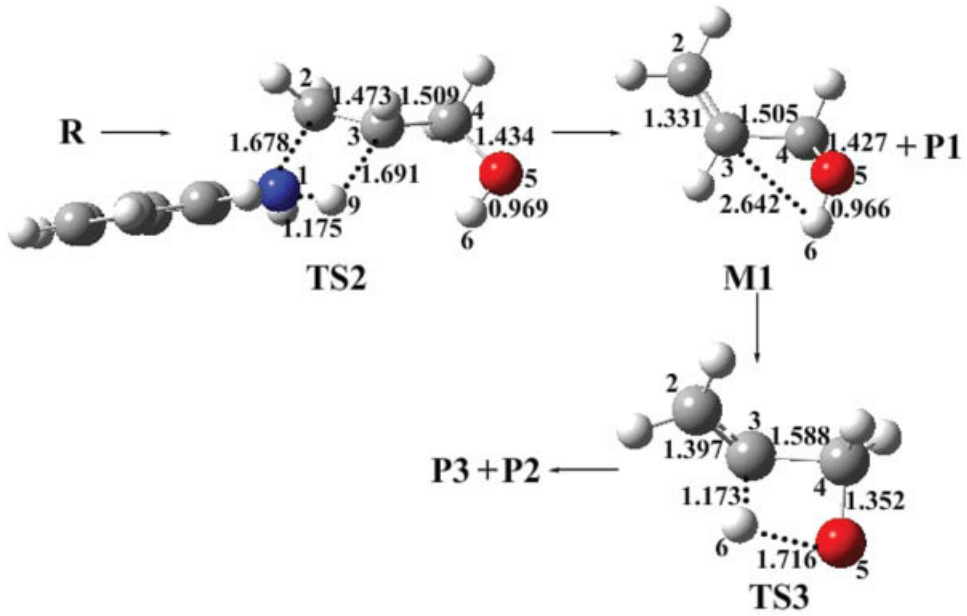

FIGURE 3. The structures and the geometrical parameters of the intermediates, transition states, and products optimized at the B3LYP/6-31G (d, p) level in channel 2 (bond length in Å).

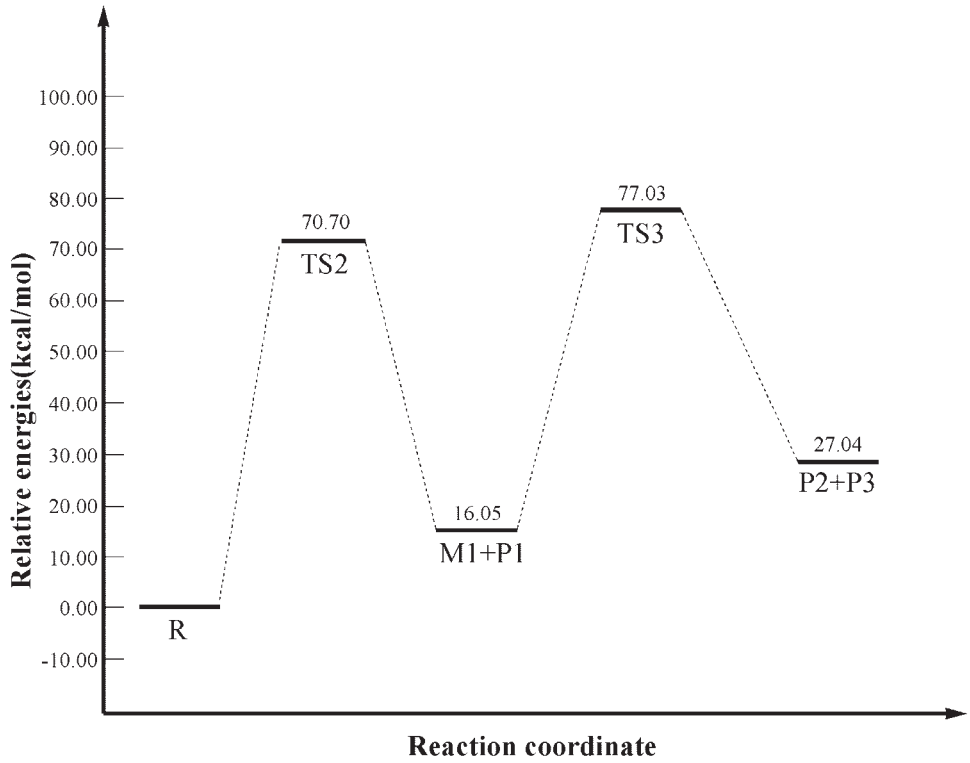

FIGURE 4. The potential energy profile of channel 2.

Å in TS4, respectively (shown in Fig. 5). The activation energy barrier of channel 3 is 89.49 kcal/mol at B3LYP/6-31G (d, p) level (shown in Fig. 6). The energy barrier of channel 3 is 35.01 kcal/mol higher than that of channel 1 and 12.46 kcal/mol higher than that of the rate-determining step in reaction channel 2, which means the reaction channel 1 is the most dominant of these three channels. The difference between the activation energy barrier of channel 2 and channel 3 is small, and so they have the same chance to occur.

REACTION CHANNEL 4

The potential energy profile of reaction channel 4 is shown in Figure 8: first, reactant R pyrolytically decomposes into P4 and intermediate M by traversing TS5, and then P5 is formed by the isomerization reaction step of intermediate M. In the first step of reaction channel 4, the bonds C(2)—C(3), C(4)—H(11), and O(5)—H(6) break, and N(1)—H(6), C(3)—H(11), and C(4)═O(5) bonds form. The bond lengths of the C(2)—C(3),

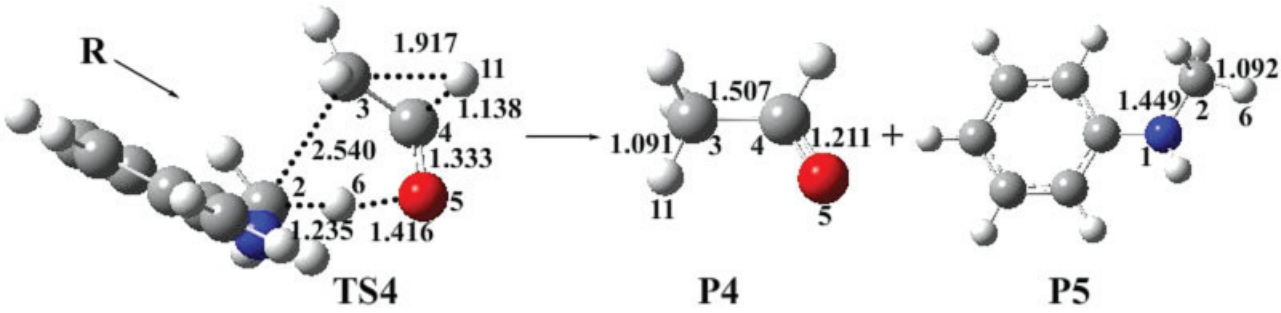

FIGURE 5. The structures and the geometrical parameters of the transition state and products optimized at the B3LYP/6-31G (d, p) level in channel 3 (bond length in Å).

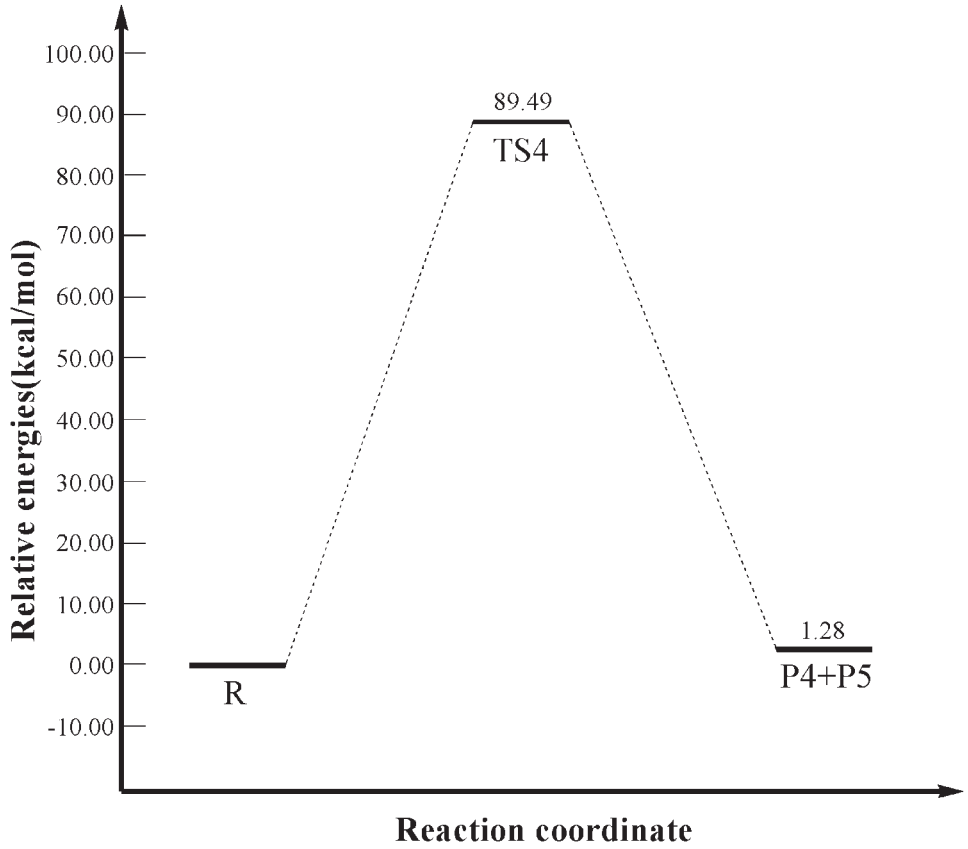

FIGURE 6. The potential energy profile of channel 3.

C(4)—H(11), O(5)—H(6), N(1)—H(6), C(3)—H(11), and C(4)—O(5) change from 1.537, 1.096, 0.972, 2.085, 2.164, and 1.416 Å in R to 2.312, 1.491, 1.695, 1.057, 1.421, and 1.267 Å in TS5, respectively (shown in Fig. 7). The activation energy barrier for the first step of channel 4 is 104.74 kcal/mol at B3LYP/6-31G (d, p) level (shown in Fig. 8). In the second step, N(1)—H(6) bond breaks while C(2)—H(6) forms. The bond lengths of the N(1)—H(6) and C(2)—H(6) change from 1.022 and 2.058 Å in M to 1.092 and 1.493 Å in TS6, respectively (shown in Fig. 7). Similar to channel 1, formation of the intermediate M in channel 4 should also traverse a transition state TS5 containing a six-membered ring, but TS5 is not the same as TS1 completely because it still contains a triatimic cycle. According to the calculation results, in the second step of reaction channel 4, the activation energy barrier of H(6) transferring from N(1) to C(2) to produce P5 by M traversing TS6 is 10.83 kcal/mol (shown in Fig. 8). In channel 4, the energy barrier of the first step is 50.26 kcal/mol higher than that of the step of directly traversing TS1 in reaction channel 1, and so this reaction step is difficult to occur commonly. And as it is 27.71 kcal/mol higher than the step of M1 traversing TS3 in reaction channel 2 and 15.25 kcal/mol higher than channel 3 which has the same pyrolytic products with it, channels 2 and 3 have more advantages than channel 4, and channel 4 is the most difficult to occur in all reaction channels.

As summarized in Table I, it gives the energy of the reactant, intermediates, transition states, and products at B3LYP/6-31G (d, p), and the energy after ZPE correction.

According to the vibration analysis of the reactant, intermediates, transition states, and the products, we know that each transition state has only one imaginary frequency (Table II), but the reactant, intermediates, and products do not have any imaginary frequency.

Channels 1 and 2 have the same pyrolysates, while channels 3 and 4 have the same pyrolysates. Channels 1 and 3 are the direct concerted reaction in which hydrogen transferring and bonds breaking occur synchronously. As one-step reaction, the

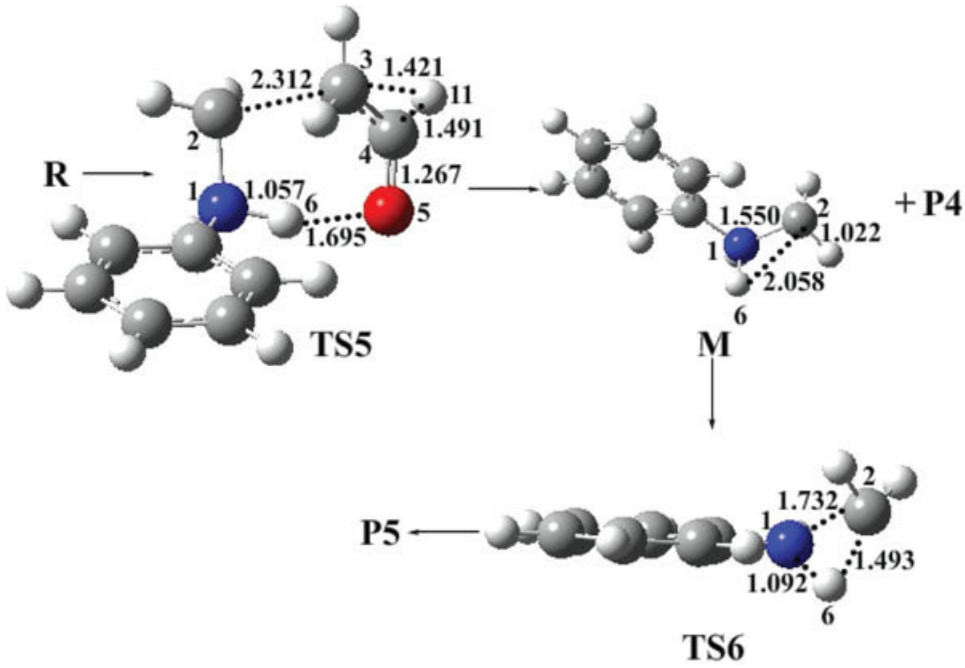

FIGURE 7. The structures and the geometrical parameters of the intermediate, transition states, and products optimized at the B3LYP/6-31G (d, p) level in channel 4 (bond length in Å).

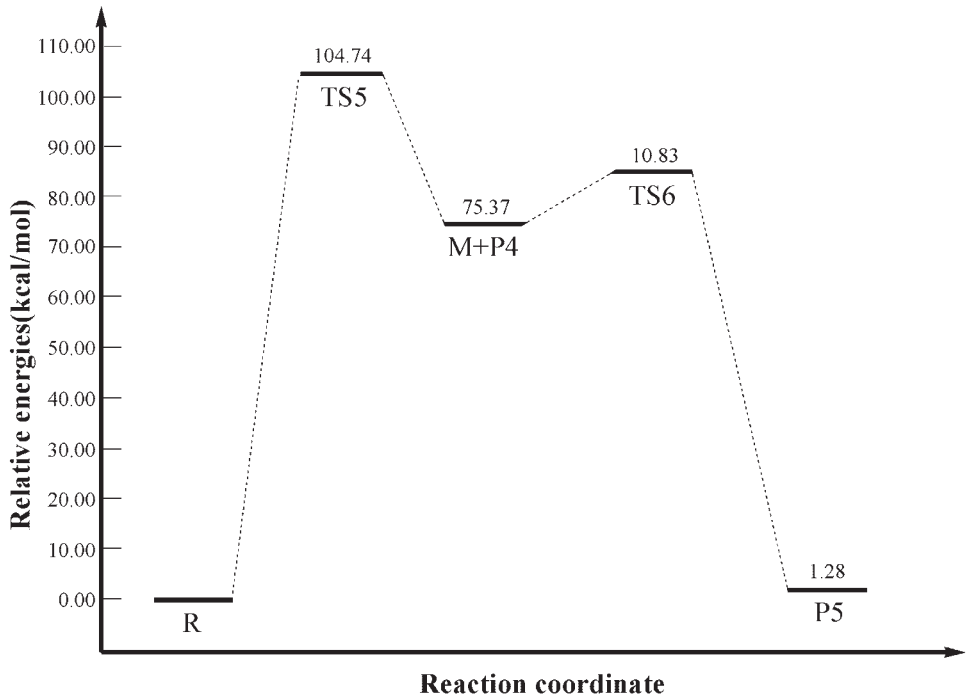

FIGURE 8. The potential energy profile of channel 4.

activation energy barrier of channel 1 is lower than that of channel 3. Channel 1 is easier to occur. Channels 2 and 4 are the step-by-step nonconcerted reactions. In channel 2, first, H(9) transferring from C(3) to N(1) and C(2)—N(1) bond breaking happen synchronously to produce intermediate M1 and P1, and later H(6) of M1 transferring from O(5) to C(3) and C(3)—C(4) bond breaking take place synchronously to P2 and P3. In channel 4, first, three processes, H(6) transferring from O(5) to N(1), H(11) transferring from C(4) to C(3), and C(2)—C(3) bond breaking, take place synchronously to form intermediate M and P4, and later M transforms to P5. Compared with that of channel 3, the activation energy barrier of the reaction channel 2's rate-determining step is lower, so this reaction channel occurs easily in these two channels. With the same pyrolytic products of different channels, on the basis of our calculation results, we can see that the activation energy barrier of the direct synergistic reaction is lower, and therefore, this channel is easier to occur, which is coincident with the experimental results [5, 8], though it is not consistent with the point of view that the energy barrier of the nonconcerted reaction pathway is lower than that of the direct concerted reaction [16–21]. In all the channels, we conclude that the energy barrier of the pyrolysates P1, P2, and P3 is lower than that of pyrolysates P4 and P5, so this kind of reaction is generally easier to occur. However, the total energy of the products is higher than that of reactant, which confirms that this pyrolytic reaction is an endothermic reaction, and this is consistent with the experiment. The change in bond energy in this reaction is also coincident with the experimental outcomes.

TABLE I

Energy of the reactant, intermediates, transition states, and products at B3LYP/6-31G (d, p) level (unit: a.u.).

Species	ZPE	B3LYP/6-31G(d,p)(ZPE)
R	0.208766	−480.561693
TS1	0.202334	−480.474542
TS2	0.199232	−480.448598
TS3	0.139129	−192.913522
TS4	0.200247	−480.418545
TS5	0.079311	−480.394144
TS6	0.196858	−326.643660
M	0.143981	−326.660990
M1	0.084994	−193.036089
P1	0.117227	−287.499277
P2	0.051124	−78.542683
P3	0.026719	−114.476480
P4	0.055597	−153.780133
P5	0.145571	−326.779508

TABLE II

Imaginary frequencies of the transition states at B3LYP/6-31G (d, p) level.

	Frequencies
TS1	548.809i
TS2	1,462.53i
TS3	883.937i
TS4	989.275i
TS5	1,065.12i
TS6	1,154.62i

Conclusions

This article studies the four reaction channels of the title compound 3-anilino-1-propanol R's gas-phase pyrolysis with the products aniline P1, ethylene P2, and formaldehyde P3 or *N*-methyl aniline P4 and aldehyde P5. All the four reaction channels are concerted reactions in which H transferring is always accompanied with bonds being broken.

In all reaction channels, reaction channel 1 has the lower activation barrier than the other three reaction channels, and, hence, we think it should be the main reaction channel of the gas-phase pyrolysis of 3-anilino-1-propanol R. The other three reaction channels' energy barriers are too high, so compared with channel 1, they are more difficult to occur.

References

1. Russell, H. F.; Bremner, J. B.; Bushelle-Edghill, J.; Lewis, M. R.; Thomas, S. R.; Bates, F., II. Tetrahedron Lett 2007, 48, 1637.
2. Gil, H.; Leygraf, C. J Electrochem Soc 2007, 154, C611.
3. Galicia, M.; Gonzalez, F. J. J Electrochem Soc 2007, 149, D46.
4. Uphoff, A.; Meffere, A.; Grotemeyer, J. In AIP Conference Proceedings, 2001; p 584.
5. Ibrahim, M. R.; Al-Awadi, N. A.; Ibrahim, Y. A.; Patel, M.; Al-Awadi, S. Tetrahedron 2007, 63, 4768.
6. Al-Awadi, S. A.; Abdallah, M. R.; Hasan, M. A.; Al-Awadi, N. A. Tetrahedron 2004, 60, 3045.
7. Al-Awadi, S. A.; Abdallah, M. R.; Dib, H. H.; Ibrahim, M.R.;

Al-Awadi, N. A.; El-Dusouqui, O. M. E. Tetrahedron 2005, 61, 5769.

8. Al-Awadi, N.; Kaul, K.; El-Dusouqui, D. J Phys Org Chem 2000, 13, 499.
9. Chen, Z. X.; Xiao, H. M. Acta Chim Sinica 1998, 56, 1198.
10. Leanikovich, A. L.; Levehik, S. V.; Halahanovich, A. L.; Lvashkevich, O. A.; Caporik, P. N. Thermochim Acta 1992, 200, 427.
11. Chen, Z. X.; Xiao, H. M. Int J Quantum Chem 2000, 79, 350.
12. Becke, A. D. J. Chem Phys 1993, 98, 5648.
13. Lee, C.; Yang, W.; Parr, R. G. Phys Rev B 1988, 37, 785.
14. Miehlich, B.; Savin, A.; Stoll, H.; Preuss, H. Chem Phys Lett 1989, 157, 200.
15. Frisch, M. J.; Trucks, G. W.; Schlegel, H. B.; Scuseria, G. E.; Robb, M. A.; Cheeseman, J. R.; Montgomery, J. A.; Vreven, T., Jr.; Kudin, K. N.; Burant, J. C.; Millam, J. M.; Iyengar, S. S.; Tomasi, J.; Barone, V.; Mennucci, B.; Cossi, M.; Scalmani, G.; Rega, N.; Petersson, G. A.; Nakatsuji, H.; Hada, M.; Ehara, M.; Toyota, K.; Fukuda, R.; Hasegawa, J.; Ishida, M.; Nakajima, T.; Honda, Y.; Kitao, O.; Nakai, H.; Klene, M.; Li, X.; Knox, J. E.; Hratchian, H. P.; Cross, J. B.; Adamo, C.; Jaramillo, J.; Gomperts, R.; Stratmann, R. E.; Yazyev, O.; Austin, A. J.; Cammi, R.; Pomelli, C.; Ochterski, J. W.; Ayala, P. Y.; Morokuma, K.; Voth, G. A.; Salvador, P.; Dannenberg, J. J.; Zakrzewski, V. G.; Dapprich, S.; Daniels, A. D.; Strain, M. C.; Farkas, O.; Malick, D. K.; Rabuck, A. D.; Raghavachari, K.; Foresman, J. B.; Ortiz, J. V.; Cui, Q.; Baboul, A. G.; Clifford, S.; Cioslowski, J.; Stefanov, B. B.; Liu, G.; Liashenko, A.; Piskorz, P.; Komaromi, I.; Martin, R. L.; Fox, D. J.; Keith, T.; Al-Laham, M. A.; Peng, C. Y.; Nanayakkara, A.; Challacombe, M.; Gill, P. M. W.; Johnson, B.; Chen, W.; Wong, M. W.; Gonzalez, C.; Pople, J. A. Gaussian 03, Revision C. 02; Gaussian, Inc.: Wallingford, CT, 2004.
16. Feng, W.; Wang, Y.; Zhang, S. Int J Quantum Chem 1997, 62, 297.
17. Jackson, E. A.; Steinberg, B. D.; Bancu, M.; Wakamiya, A.; Scote, L. T. J Am Chem Soc 2007, 129, 484.
18. Hell, R. L.; Truong, T. N. J Phys Chem 1994, 101, 10442.
19. Maguire, N. E.; McLaren, A. B.; Sweeney, J. B. Synlett 2003, 12, 1898.
20. Seebach, D. Angew Chem Int Ed Engl 1988, 27, 1624.
21. Wei, D. H.; Tang, M. S.; Wang, H. M.; Li, S.; Zhao, J.; Zhao, C. F. Acta Chim Sin 2008, 66, 321.